HHS Public Access

Author manuscript

Lab Invest. Author manuscript; available in PMC 2011 October 01.

Published in final edited form as:

Lab Invest. 2011 April ; 91(4): 488–498. doi:10.1038/labinvest.2010.188.

Expression profiles of podocytes exposed to high glucose reveal new insights into early diabetic glomerulopathy

Sanjay Jain, MD, PhD[1,2,*], **Laura De Petris, MD**[3], **Masato Hoshi, MD, PhD**[1], **Shreeram Akilesh, MD, PhD**[2], **Rajshekhar Chatterjee, PhD**[1], and **Helen Liapis, MD**[1,2,*]

[1] Department of Internal Medicine (Renal Division), Washington University, School of Medicine, St Louis, MO

[2] Department of Pathology & Immunology, Washington University, School of Medicine, St Louis, MO

[3] Department of Pediatrics, San Benedetto del Tronto Hospital, Italy

Abstract

Podocyte injury has been suggested to play a pivotal role in the pathogenesis of diabetic glomerulopathy. To glean insights intomolecular mechanisms underlying diabetic podocyte injury we generated temporal global gene transcript profiles of podocytes exposed to high glucose for a time interval of 1 or 2 weeks using microarrays. A number of genes were altered at both 1 and 2 weeks of glucose exposure compared to controls grown under normal glucose. These included extracellular matrix modulators, cell cycle regulators, extracellular transduction signals and membrane transport proteins. Novel genes that were altered at both one and two weeks of high glucose exposure included Neutrophil gelatinase-associated lipocalin (*LCN2* or *NGAL*, decreased by 3.2 fold at 1 week and by 7.2 fold at 2 weeks), Endothelial lipase (*EL*, increased by 3.6 fold at 1 week and 3.9 fold at 2 week), and UDP-glucuronosyltransferase 8 (*UGT8*, increased by 3.9 fold at 1 week and 5.0 fold at 2 weeks). To further validate these results we used real-time PCR from independent podocyte cultures, immunohistochemistry in renal biopsies and immunoblotting on urine specimens from diabetic patients. A more detailed time course revealed changes in LCN2 and EL mRNA levels as early as 6 hours and in UGT8 mRNA levels at 12 hours post-high glucose exposure. EL immunohistochemistry on human tissues showed markedly increased expression in glomeruli and immunoblotting readily detected EL in a subset of urine samples from diabetic nephropathy patients. In addition to previously implicated roles of these genes in ischemic or oxidative stress, our results further support their importance in hyperglycemic podocyte stress and possibly diabetic glomerulopathy pathogenesis and diagnosis in humans.

[*]Corresponding authors: Sanjay Jain, MD, PhD, Assistant Professor, Renal Division, Departments of Medicine, Pathology and Immunology, 660 S. Euclid Ave., Box 8126, St. Louis, MO 63110, (314)-454-8728 (O), (314)-454-8464 (lab), (314)-454-7735 (fax). Helen Liapis, MD, Washington University School of Medicine, Department of Pathology & Immunology, 660 S. Euclid Avenue, Campus Box 8118, Saint Louis, Missouri 63110-1093, Tel: (314) 362-7440, Fax: (314) 747-2040.

Disclosures : None

Keywords

diabetic glomerulopathy; podocytes; expression profiles; nephropathy

Diabetic nephropathy, a clinical syndrome of persistent microalbuminuria and a common complication of diabetes, is currently the leading cause of end-stage renal disease (ESRD) in the United States. Albuminuria indicates excessive albumin filtration from the glomerulus into the tubules which overwhelms their metabolic capacity promoting local inflammation and tubulointerstitial scarring known as diabetic nephropathy. A central initial event in the albuminuria-ESRD sequence is podocyte injury (1–3). The podocyte consists of a cell body, primary and secondary foot processes and the slit diaphragm (filtration barrier). It is proposed that hyperglycemia causes podocyte oxidative stress - defined as damage caused by reactive oxygen species- which leads to foot process effacement followed by podocyte apoptosis (4,5). For example, in the Akita model of type 1 diabetes, or the leptin receptor–deficient db/db mouse model of type 2 DKD, podocytes lose nephrin expression (the major component of the slit diaphragm), foot processes become effaced and eventually detach from the GBM undergoing death by apoptosis (4,5). Podocyte apoptosis is in part mediated by transforming growth factor-β (TGFβ) signaling and possibly epithelial-mesenchymal transformation (EMT) (6–8). For example, Li et al show that TGF-β under conditions of high glucose suppresses expression of key slit diaphragm proteins, induces extracellular matrix protein expression (e.g., fibronectin and collagen I), and leads to secretion of matrix metalloproteinase-9 (MMP-9) (8). However, activation of other metabolic pathways, for example, the polyol pathway (9), protein kinase C (10), the hexoamine pathway (11–14), also play a role in diabetic nephropathy. Recently, VEGF-mediated signaling has also been implicated in this process (15,16) and hyperglycemia mimicking hypoxic injury to endothelial cells is proposed (17,18). These studies demonstrate that the molecular pathogenesis of diabetic podocyte injury is likely multifactorial involving a number of interrelated signaling pathways that have yet to be well understood. Understanding the molecular milieu of diabetic podocyte injury, an early event in diabetic nephropathy remains a primary target in identifying novel avenues for early intervention and prevention of severe late complications of this increasingly prevalent disease.

We have previously found that BMP7 confers podocyte resistance to hyperglycemic injury by restoring major podocyte proteins such as synaptopodin and podocin (19). Identifying new molecular changes and integrating them to known pathways are important inobtaining deeper insights into the mechanism of diabetic nephropathy, early diagnosis and possible new therapies. One approach towards this end is using high throughput methods that detect multiple molecular changes simultaneously. For example, microarray technology enables one tomeasure gene expression in whole genomes to identify new genes and pathways associated with a disease. Microarray studies on whole diabetic kidney and/or on mesangial cells, have found altered gene expression in the early phases of diabetic injury in mice (20–24). While these studies provide initial insights into early global changes in the diabetic kidney, little is known about the molecular and temporal events occurring specifically in podocytes. Recently, early global changes due to high glucose were reported in podocytes (25). Information regarding the molecular changes in podocytes due to prolonged high

glucose exposure will help derive important insights into how these may lead to diabetic nephropathy, a disease that develops over a long time. This will also enhance the possibility of discovering biomarkers that can help discern podocyte dysfunction over broad range of this disease.

The aim of this study was to examine the effect of prolonged high glucose exposure on mRNA expression profiles in mouse podocytes. Using expression microarrays we discovered genes that are strongly and consistently associated with hyperglycemic podocyte stress in a time-course analysis. The in vitro podocyte injury alterations were also detected in renal biopsies and urine samples from patients with diabetic nephropathy suggesting that these may be relevant to the pathogenesis of diabetic glomerular disease in humans.

Methods

Cell Culture

Experiments were performed using a thermosensitive SV-40-transfected immortalized mouse podocyte cell line (gift from Peter Mundel, Mount Sinai School of Medicine, New York). Podocytes were cultured in RPMI 1640 supplemented with 10% fetal bovine serum (FBS), 100 U/mL penicillin, and 100 μg/mL streptomycin. Cells were grown at 33° C and treated with 10 U/mL of mouse recombinant -interferon (Sigma, St. Louis, Mo, USA) as previously described (19). At confluence podocytes were maintained on a bed of type I collagen at 37° C for 14 days without γ-interferon to allow differentiation (26). These conditionally immortalized cells were then either exposed to media containing normal glucose (NG) as a control (5.5 mmol/L D-glucose) or High Glucose (HG) (25 mmol/L D-glucose) for 6, 12, 18, 24, 72 hours and one or two weeks. Experiments were performed in duplicate.

To account for the osmotic effect of high glucose, podocytes were starved for 24 hours with media containing mannitol. In this model, 1 week exposure to HG was considered an arbitrary representation of sub-acute HG stress and an arbitrary representation of sustained stress was taken as HG exposure for 2 weeks. Exposure of podocytes to HG from 6–72 hours was performed to study temporal alterations and to independently validate the microarray results.

RNA extraction

Total RNA was extracted with TRIzol reagent according to manufacturer's protocol (Invitrogen Inc.). An additional cleanup step was used by employing an RNeasy Mini Kit (QIAGEN Inc., Valencia, CA, USA). RNA concentration and purity was assessed by spectroscopy (nanodrop) with the A260/A280 ratio in the range 1.77–2.08. RNA samples were used immediately or stored at −80° C for subsequent microarray analysis or for Real-time PCR.

Microarray hybridization and data analysis

Total RNAs (1–5 μg) extracted from podocytes cultured in HG for 1 or 2 weeks and in NG for 2 weeks (in duplicate) were reverse-transcribed into cDNA and biotin-labeled cRNA

targets were generated. The cRNA was fragmented and hybridized to Affymetrix GeneChip Mouse Genome 430 2.0 microarrays (Affymetrix, Santa Clara, CA, USA) at the Laboratory of Translational Pathology Microarray Core Facility of Washington University as previously described (27). Quantitative analysis of hybridization patterns and intensities was performed by Affymetrix software, and the resulting data were analyzed by Affymetrix Microarray Suite software (Version 5.0). The entire raw data are available at http://bioinformatics.wustl.edu. The data were scaled to 1500 units of signal intensity for comparisons across samples and imported into dCHIP for analysis. The data were filtered to exclude genes that were not expressed or did not vary using the coefficient of variation (standard deviation/mean) and percentage of presence calls in the arrays. First, the genes were filtered such that the coefficient of variation across samples was greater than 0.5 and less than 1000 (28,29). Second, only the genes that had a presence call percentage of ≥20% across the arrays were included for analysis. After filtering, a list of 1,790 genes was used to identify differentially expressed genes in the dataset. Using the replicate NG arrays as the baseline (B), the replicate 1W or 2W array experiments (E) were each compared for changes in gene expression using a 3-fold cutoff (B/E or E/B>3), absolute signal difference >100 (B-E or E-B>100) and a presence call percentage of ≥20% in each of the baseline and experimental datasets. The raw signal intensity data for the resulting differentially expressed genes were reviewed and only those genes that showed close agreement between the duplicates were pursued.

Real-time PCR

Total RNA extracted from podocytes cultured (duplicates) in NG or HG in various time intervals (6hrs to 2 weeks) was converted into cDNA and amplified by real-time polymerase chain reaction (PCR) in “one-step” reaction (Qiagen, OneStep RT-PCR, Germantown, MD, USA). The SYBR Green was used as fluorogenic probe system. PCR kinetics and data quantification was performed with 4000 Multiplex Quantitative PCR System Software (Stratagene, La Jolla, CA). Quantification of the target gene was performed according to the standard curve method (30). mRNA levels were normalized to β-actin. Experiments were performed in triplicate. We used the following primers: Ugt8 5’CCCACTGCCAGAAGATCTGC-3’; 3’-TGGAATAGCAAGGGCTGCTAA-5’; EL 5’-GAGCGAGCCGTACACCTCTT-3’, 3’-TGGATACGCTGGCAACTTTG-5’; LCN 5’-GATGCGCAGAGACCCAATG-3’, 3’-AGGAACGTTTCACCCGCTTT-5’.

Human tissue studies

Paraffin-embedded tissue blocks or fresh cryopreserved tissue from renal biopsies from patients (n=8) with diabetic glomerulosclerosis were randomly retrieved from the files of the Department of Pathology and Immunology at Washington University in St. Louis or George M. O’Brien Center for Kidney Disease Research Kidney Translational Research Core at Washington University. All specimens used for research were collected under protocols approved by the Institutional Review Board of Washington University School of Medicine. Light microscopy, routine immunofluorescence and electron microscopy were retrospectively reviewed to ascertain diagnosis. Seven controls consisted of histologically normal non-diabetic kidneys.

Immunohistochemistry

Immunohistochemistry on formalin-fixed paraffin-embedded sections (4μm) was performed using antigen retrieval for 15 minutes (10mM sodium citrate, 0.05% Tween20, pH 6.0) and peroxidase method. Hematoxylin-Eosin was used for counterstaining. For cryopreserved tissue, immunofluorescence was performed on 10 μm sections that were post-fixed in PBS containing 4% paraformaldehyde, washed and blocked with Image-iT^{TM} FX signal enhancer (Invitrogen Inc.) for 30 minutes and then incubated with the primary antibody. The primary and secondary antibodies used were anti-endothelial lipase (1:50, Cayman chemical company Cat# 100030) and biotinylated anti-rabbit (1:200, JacksonImmunoresearch Inc.), respectively. WT1 antibody (1:10, Santa Cruz Biotechnology Inc.) was used to label podocytes in biopsies. The signals were visualized using streptavidin-HRP (1:400, JacksonImmunoresearch Inc.) for paraffin embedded tissue, and with streptavidin-alexa594 (molecular probes) for EL immunofluorescence, and strepatavidin-alexa488 for WT1 immunofluorescence. Slides were incubated with bis-Benzamide (Sigma) for 5 minutes to visualize nuclei. Nikon 80i upright microscope (Nikon) equipped with CoolSnapES camera (photometrics) was used to capture the images and Nikon Elements (Nikon)and Adobe Photoshop (Adobe) softwares were used for image processing.

Immunoblotting

SDS-PAGE (10%) was performed on urine specimens (15μl each) of 4 patients with diabetic nephropathy and 3 individuals with no known kidney disease (controls) using standard procedures, The proteins were transferred to PVDF membrane using Bio-Rad semi-dry apparatus. After washing twice with TBS buffer, the PVDF membrane was blocked using 2% non-fat milk and 2% BSA in TBST buffer for 1 hour at room temperature, and then incubated with rabbit anti-endothelial lipase (1:100) and mouse anti-albumin (1:2000, Invitrogen Cat#03-0700) antibodies for 16 hours at 4° C. After washing with TBST, the membranes were incubated for 1 hour at 25° C with IRDye800CW-conjugated goat anti-rabbit IgG (1:2000, red) and IRDye680-conjugated goat anti-mouse IgG (1:2000, green) secondary antibodies (LI-COR Biosciences). After washing, the respective antigens were visualized on an Odyssey Infrared Imaging System (LI-COR Biosciences) with both 700- and 800-nm channels. For confirming specificity of EL antibody different amounts of purified human Albumin (Sigma) ranging from 0.1μg to 50μg were blotted on two separate nitro-cellulose membranes and immunoblotting and detection was performed as described above for albumin and EL.

Statistical Analysis

In real-time PCR experiments a two-way analysis of variance (ANOVA) was used to compare control with experimental groups. Results are shown as the mean ± SD. $P < 0.05$ was considered statistically significant.

Results

To identify podocyte-specific genes potentially regulated by HG exposure we treated podocytes in culture for one or two weeks with HG and compared their expression profiles with controls grown in NG for two weeks using Affymetrix Mouse Genome 430 2.0

microarrays. A filtered set of 1,790 genes was examined for changes in gene expression. Compared to NG there were 19 transcripts that were significantly downregulated at 1 week of HG exposure (Tables 1 and 2, see methods). These include: brain expressed gene 1 (Bex1), Thyroid hormone receptor interactor 11 (Trip11) and lipocalin 2 (Lcn2). There were 19 transcripts that were up–regulated at 1 week including interleukin 1 receptor-like 1 (Il1rl1), endothelial lipase (Lipg or EL) and UDP galactosyltransferase 8A (Ugt8). Twenty five genes were downregulated in week 2, including Lcn2, matrix metalloproteinase 2 (Mmp2) and Cyclin 1 (Ccni). Thirty two genes were upregulated at 2 weeks in HG treated podocytes including Ugt8 and endothelial lipase (for detailed list and fold changes see Table 1).

We next focused on identifying genes that were represented by probesets showing consistent changes in response to HG at both 1 week (arbitrary representation of sub-acute HG stress) and 2 weeks (arbitrary representation of sustained HG stress) in our model. We were interested in this for two reasons. First, these could represent potential biomarkers that remain altered in diabetic glomerular disease. Second, these could provide insights into possible mechanisms underlying HG-mediated podocyte dysfunction. Therefore, we generated a gene list representing intersection of differentially expressed genes at both 1 and 2 weeks of HG compared to NG exposure (Table 3). Of the ten genes that were differentially expressed in both the 1 week and 2 week time points compared to the normal glucose control, only three genes showed consistent changes in probesets across replicates when the raw signal intensity data were examined, and that had defined annotation information. These include neutrophil gelatinase-associated lipocalin (*Lcn2* also known as *Ngal1*) whose expression was decreased in response to high glucose, and endothelial lipase (*EL*) and UDP-glucuronosyltransferase 8 (*Ugt8*) whose expression levels increased in response to high glucose (Figure 1).

To further understand the temporal dynamics of these alterations, and independently validate microarray results, we isolated RNA from podocytes exposed to HG at different time intervals (6h, 12h, 18h, 24h, 72h, 1 weeks and 2weeks) and performed RT-PCR for Lcn2, EL and Ugt8 (Figure 2). Consistent with our microarray data we found that all three genes were modulated by HG. Importantly, Lcn2 levels started to decrease as early as 6 h after HG exposure and were significantly down regulated by HG at 18 hours. By 72h Lcn2 was barely detectable and remained low for the remaining time points of this experiment and up to 1 and 2 weeks (Figure 2a). EL was upregulated as early as 6 hours by HG and increased by 3 and 10 fold at 1 week and 2 weeks, respectively, compared to control (Figure 2b). Ugt8 was upregulated by HG as early as 12 hours and remained elevated at 2 weeks of HG exposure (Figure 2c). These results validate the microarray findings and demonstrate that perturbation in expression of these genes after high glucose exposure was a relatively early event (less than 18 h after HG exposure) and the expression remained downregulated (for Lcn2) or upregulated (for EL and Ugt8) at longer times of HG exposure.

We next determined if the HG responsive genes found from experiments in vitro were also altered in patients with diabetic nephropathy. To obtain a clearer idea at a cell specific level we resorted to immunohistochemistry in kidneys from diabetic or non-diabetic patients (8 diabetic and 7 non-diabetic controls). Among the three differentially expressed genes, we

focused on EL2 as Ugt8 antibodies were not available and Lcn2 was barely detectable in podocytes of non-diabetic patients (low abundance expression) thus rendering it unsuitable for detecting any further downregulation in situ in diabetic glomeruli. Consistent with our cell-culture results, we observed markedly higher EL2 expression in podocytes of almost all diabetic nephropathy patients (7 out of 8) compared to those from non-diabetics (normal) (Figure 3). Immunostaining with WT1 and EL antibodies using immunoperoxidase or immunofluorescence methods confirm high expression of EL in podocytes of diabetic glomeruli. Parietal cells of diabetic glomeruli also exhibit high EL immunopositivity compared to controls and non diabetic kidneys, but the significance of this is unclear.

We further examined if these findings can have potential utility in DN diagnosis and performed EL immunoblotting in urine samples from diabetic nephropathy and non-diabetic control patients EL was readily detected in urine of a subset of DN patients (2/4), while none of the control patients (3/3) show EL expression (Fig. 4).

Discussion

We have employed microarray analysis to delineate potential molecular pathways underlying podocyte injury in diabetic glomerulopathy using an in vitro model and confirmed a subset of the observed in vitro changes in independent time-course experiments and in specimens from humans with diabetic nephropathy. Out of a total of 95 transcripts that were differentially expressed upon HG exposure of 1 or 2 weeks, we found that three remained altered at both 1 and 2 weeks (*Lcn2*, *Ugt8* and *EL*) suggesting that these are promising candidates as biomarkers or potential contributors to the pathogenesis of diabetic glomerular disease. Time course RT-PCR experiments revealed that changes in mRNAs of these genes occurs shortly after exposure to high glucose and remain altered that may have implications in early and late detection and pathogenesis.

We discovered that *Lcn2* expression exhibited a time-dependent decrease in podocytes beginning as early as 6 h after HG treatment. LCN2 is a member of the lipocalinsuperfamily that forms a complex with iron-binding siderophores. This complex plays a role during nephrogenesis by promoting the conversion of renal progenitorsinto tubules (31). Further, it is also highly upregulated in tubular cells after acute kidney injury (32). These results support the idea that upregulation of Lcn2 is important for survival or regeneration after injury from stress. This idea is further supported by the observation that recombinant Lcn2 reduces proximal tubular injury in an ischemia reperfusion injury model by inhibiting apoptosis (33). The decreased expression of Lcn2 observed in our study was unexpected considering its upregulation in other injury models, however, our independent validation using quantitative RTPCR at several time points supported the observed Lcn2 downregulation upon HG exposure . This observation suggests that failure of podocytes to sustain normal or high levels of Lcn2 after HG exposure may be a potential mechanism of podocyte injury and apoptosis induced by HG. LCN2 also binds to matrix metalloproteinase-9(MMP-9) and protects this extracellular matrix remodeling enzymefrom autodegradation (34). Whether reduced expression of LCN2 contributes to glomerular basement membrane (GBM) thickening and extracellular matrix accumulation (hallmark

lesions of diabetic glomerulosclerosis) by increasing autodegradation of MMP-9 or other metalloproteinases remains to be seen.

Our discovery of upregulation of Endothelial lipase (EL) in vitro and in human samples have important clinical implications. EL, the most recently discovered member of the lipase gene family is an important negative modulator of high density lipoprotein (HDL). EL is also involved in inflammatory state by promoting monocyte adhesion to the vascular endothelium (35, 36). Recent data indicate that HDL inhibits apoptosis, lipid oxidation, cytokine and adhesion molecule production (37). Since in vitro and in vivo studies have linked HDL to both diabetes mellitus and inflammation, it is possible that increased EL in our study of podocyte HG exposure may be a mechanism of HDL-mediated or cytokine-mediated effects in diabetic glomerulopathy. Further, HDL is thought of as protective against formation of extrarenal vascular calcifications, a common and serious complication in patients with chronic kidney disease (38). Therefore, it is possible that elevated EL in diabetic glomerulopathy mediates low HDL-associated increased vascular calcifications. Importantly, we demonstrate for the first time that podocytes may be a significant source of EL, a protein normally secreted by vascular endothelial and smooth cells or macrophages (cell types typically not present in the glomerulus), after HG exposure. Because our studies show that EL can be readily detected in human urine samples in a subset of diabetic patients also supports its potential use in diabetic nephropathy diagnosis. Further large scale studies are warranted to determine the diagnostic utility of aberrant EL expression in diabetic and non-diabetic nephropathy at different stages of the disease.

While Lcn2 and EL can be potentially linked to HG mediated changes related to diabetic nephropathy, currently no such information is available for Ugt8. Ugt8 consists of a super family of enzymes that catalyze glucuronidation (39). In particular Ugt8 family catalyzes the transfer of galactose to ceramide, a key enzymatic step in the biosynthesis of galactocerebrosides. Galactocerebrosides are abundant sphingolipids of the myelin membrane of the central and peripheral nervous system (40), and Ugt8 is also present in the kidney during metanephric development (41). Ugt8 deficiency results in a spectrum of neurological symptoms characterized by tremors, ataxia, progressive hindlimb paralysis and vacuole formation in ventral spinal cord (42). Increased ceramide levels have also been shown to increase apoptosis in a number of systems (43). On the other hand, Ugt8 upregulation is associated with increased metastatic potential to lung by specifically enhancing the ability to metastasize to, colonize and survive within the lung (44). It should be noted that podocytes have been touted as neuronal counterparts in the kidney and the increased Ugt8 levels may be protective compensatory response to prevent podocyte degeneration by enhancing their survival, perhaps similar to its role in the nervous system by regulating lipid metabolism. Future studies would be needed to explore a potential relationship of Ugt8 to diabetic glomerulopathy or podocyte function.

In conclusion, our study identified podocyte specific genes that are regulated by acute and sustained HG exposure. While some of these have been previously associated with diabetic glomerulopathy thus validating our strategy, we found several novel ones. We confirmed a subset of these that may cause deranged lipid metabolism and impaired injury response in podocytes and contribute to diabetic nephropathy. Further, we show data for potential

application of these in diagnosis of diabetic nephropathy in human specimens. Thus these studies provide new molecular insights into the role of podocytes in diabetic renal disease and support the notion that diabetes with regards to the glomerulus is another podocytopathy (45).

Acknowledgments

We thank Amanda Knoten, Angela Lluka and Adee Heiman for excellent technical assistance and Mary Hoffman, Jessica Vanwinkle and Daniel Martin for human specimen processing and acquisition. We thank Dr. George Jarad for human purified albumin and albumin antibodies. We are grateful to Mark Watson and Laboratory of Translational Pathology at Washington University School of Medicine for providing core services for microarray and laser capture microscopy studies, and to Dr. Erwin P. Bottinger for providing laboratory resources to culture podocytes for RT-PCR experiments.

This work was partly supported by Core services provided by an NIH George M. O'Brien Center for Kidney Disease Research grant (P30-DK079333) to Washington University, NIH grant DK081644 (to S. Jain) and interdepartmental research funds to H. Liapis. Part of this work was presented in an abstract form at the annual United States and Canadian Academy of Pathology (USCAP) 2006 and International Podocyte Conference (2006).

Abbreviations

EL	endothelial lipase
ESRD	end-stage renal disease
HDL	high density lipoprotein
HG	high glucose
NG	normal glucose

References

1. Wolf G, Chen S, Ziyadeh FN. From the periphery of the glomerular capillary wall toward the center of disease: podocyte injury comes of age in diabetic nephropathy. Diabetes. 2005; 54:1626–1634. [PubMed: 15919782]
2. Reddy GR, Kotlyarevska K, Ransom RF, Menon RK. The podocyte and diabetes mellitus: is the podocyte the key to the origins of diabetic nephropathy? Curr Opin Nephrol Hypertens. 2008; 17:32–36. [PubMed: 18090667]
3. Marshall MS. The podocyte: a major player in the development of diabetic nephropathy? Horm Metab Res. 2005; 37(suppl 1):9–16. [PubMed: 15918105]
4. Susztak K, Raff AC, Schiffer M, Bottinger EP. Glucose-induced reactive oxygen species cause apoptosis of podocytes and podocyte depletion at the onset of diabetic nephropathy. Diabetes. 2006; 55:225–233. [PubMed: 16380497]
5. Stitt-Cavanagh E, MacLeod L, Kennedy C. The podocyte in diabetic kidney disease. ScientificWorldJournal. 2009; 9:1127–39. [PubMed: 19838599]
6. Ziyadeh FN. Different roles for TGF-beta and VEGF in the pathogenesis of the cardinal features of diabetic nephropathy. Diabetes Res Clin Pract. 2008; 82 (Suppl 1):S38–41. [PubMed: 18842317]
7. Schiffer M, Mundel P, Shaw AS, Bottinger EP. A novel role for the adaptor molecule CD2-associated protein in transforming growth factor-beta-induced apoptosis. J Biol Chem. 2004; 279:37004–37012. [PubMed: 15213232]
8. Li Y, Kang YS, Dai C, Kiss LP, Wen X, Liu Y. Epithelial-to-mesenchymal transition is a potential pathway leading to podocyte dysfunction and proteinuria. Am J Pathol. 2008; 172(2):299–308. [PubMed: 18202193]
9. Marrero B, Amy K. Banes-Berce. Role of the JAK/STAT signaling pathway in diabetic nephropathy. Am J Physiol Renal Physiol. 2006; 290:F762–F768. [PubMed: 16527921]

10. Noh H, King GL. The role of protein kinase C activation in diabetic nephropathy. Kidney Int Suppl. 2007 Aug.(106):S49–53. [PubMed: 17653211]
11. Forbes JM, Fukami K, Cooper ME. Diabetic nephropathy: where hemodynamics meets metabolism. Exp Clin Endocrinol Diabetes. 2007 Feb; 115(2):69–84. [PubMed: 17318765]
12. Schleicher ED, Weigert C. Role of the hexosamine biosynthetic pathway in diabetic nephropathy. Kidney Int Suppl. 2000 Sep.77:S13–8. [PubMed: 10997685]
13. Daniels MC, McClain DA, Crook ED. Transcriptional regulation of transforming growth factor beta1 by glucose: investigation into the role of the hexosamine biosynthesis pathway. Am J Med Sci. 2000 Mar; 319(3):138–42. [PubMed: 10746823]
14. Goldberg HJ, Whiteside CI, Fantus IG. The hexosamine pathway regulates the plasminogen activator inhibitor-1 gene promoter and Sp1 transcriptional activation through protein kinase C 1 and. J Biol Chem. 2002; 277:33833–33841. [PubMed: 12105191]
15. Müller-Deile J, Worthmann K, Saleem M, Tossidou I, Haller H, Schiffer M. The balance of autocrine VEGF-A and VEGF-C determines podocyte survival. Am J Physiol Renal Physiol. 2009; 297(6):F1656–67. [PubMed: 19828679]
16. Satchell SC, Harper SJ, Tooke JE, Kerjaschki D, Saleem MA, Mathieson PW. Human podocytes express angiopoietin 1, a potential regulator of glomerular vascular endothelial growth factor. J Am Soc Nephrol. 2002; 13(2):544–50. [PubMed: 11805186]
17. Li JM, Shah AM. ROS generation by nonphagocytic NADPH oxidase: potential relevance in diabetic nephropathy. J Am Soc Nephrol. 2003; 14 (8 Suppl 3):S221–6. [PubMed: 12874435]
18. Nyengaard JR, Ido Y, Kilo C, Williamson JR. Interactions between hyperglycemia and hypoxia: implications for diabetic retinopathy. Diabetes. 2004; 53(11):2931–8. [PubMed: 15504974]
19. De Petris L, Hruska KA, Chiechio S, Liapis H. Bone morphogenetic protein-7 delays podocyte injury due to high glucose. Nephrol Dial Transplant. 2007 Dec; 22(12):3442–3450. [PubMed: 17686813]
20. Fan Q, Shike T, Shigehara T, Tanimoto M, Gohda T, Makita Y, Wang LN, Horikoshi S, Tomino Y. Gene expression profiles in diabetic KK/Ta mice. Kidney Int. 2003; 64:1978–1985. [PubMed: 14633120]
21. Wilson KH, Eckenrode SE, Li QZ, Ruan QG, Yang P, Shi JD, Davoodi-Semiromi A, McIndoe RA, Croker BP, She JX. Microarray analysis of gene expression in the kidneys of new- and post-onset diabetic NOD mice. Diabetes. 2003; 52:2151–2159. [PubMed: 12882935]
22. Susztak K, Bottinger E, Novetsky A, Liang D, Zhu Yanqing Ciccone E, Wu D, Dunn S, McCue P, Sharma K. Molecular profiling of diabetic mouse kidney reveals novel genes linked to glomerular disease. Diabetes. 2004; 53:784–794. [PubMed: 14988265]
23. Baelde HJ, Eikmans M, Doran PP, Lappin DW, de Heer E, Bruijn JA. Gene expression profiling in glomeruli from human kidneys with diabetic nephropathy. Am J Kidney Dis. 2004; 43:636–650. [PubMed: 15042541]
24. Morrison J, Knoll Kristen, Martin J, Liang Hessnerand Mingyu. Effect of high glucose on gene expression in mesangial cells: upregulation of the thiol pathway is an adaptational response. Physiol Genomics. 2004; 17:271–282. [PubMed: 15039483]
25. Han SH, Yang S, Jung DS, Li JJ, Kim JJ, Kwak SJ, Kim DK, Moon SJ, Lee JE, Han DS, Kang SW. Gene expression patterns in glucose-stimulated podocytes. Biochem Biophys Res Commun. 2008 Jun 6; 370(3):514–8. [PubMed: 18395008]
26. Mundel P, Reiser J, Zúñiga Mejía Borja A, et al. Rearrangements of the cytoskeleton and cell contacts induce process formation during differentiation of conditionally immortalized mouse podocyte cell lines. Exp Cell Res. 1997; 236:248–258. [PubMed: 9344605]
27. Jain S, Suarez AA, McGuire J, Liapis H. Expression profiles of Renal Dysplasia Reveal New Insights in renal Development and Disease. Pediatric nephrology. 2007; 22(7):962–974. [PubMed: 17450386]
28. Jains, A.; Dubes, R. Algorithms for clustering data. Prentice-Hall; Englewood Cliffs NJ: 1988.
29. Li; Wong; Li, Cheng; Wong, Wing Hung. Model-based analysis of oligonucleotide arrays: Expression index computation and outlier detection. PNAS. Jan 2; 2001 98(1):31–36. [PubMed: 11134512]

30. Livak KJ, Schmittgen TD. Analysis of relative gene expression data using real-time quantitative PCR and the $2^{-\Delta\Delta Ct}$ method. Methods. 2001; 25:402–408. [PubMed: 11846609]
31. Challen GA, Martinez G, Davis MJ, Taylor DF, Crowe M, Teasdale RD, Grimmond SM, Little MH. Identifying the molecular phenotype of renal progenitor cells. J Am Soc Nephrol. 2004; 5:2344–2357. [PubMed: 15339983]
32. Mishra J, Ma Q, Prada A, Mitsnefes M, Zahedi K, Yang J, Barasch J, Devarajan P. Identification of neutrophil gelatinase-associated lipocalin as a novel early urinary biomarker for ischemic renal injury. J Am Soc Nephrol. 2003; 14:2534–2543. [PubMed: 14514731]
33. Yan L, Borregaard N, Kjeldsen L, Moses MA. The high molecular weight urinary matrix metalloproteinase activity is a complex of gelatinase B/MMP-9 and neutrophil gelatinase-associated lipocalin (NGAL). J Biol Chem. Oct; 2005 276 (40):37258–37265. [PubMed: 11486009]
34. Paradis ME, Badellino KO. Endothelial lipase is associated with inflammation in humans. Journal of Lipid Research. Dec.2006 47:2808–2813. [PubMed: 16980590]
35. Broedl UC, Maugeais C. Effects of Nonlipolytic Ligand Function of Endothelial Lipase on High Density Lipoprotein Metabolism in Vivo. J Biol Chem. Oct; 2003 278 (42):40688–40693. [PubMed: 12909635]
36. Ruge T, Neuger L. Lipoprotein lipase in the kidney: activity varies widely among animal species. Am J Physiol Renal Physiol. 2004; 287:F1131–F1139. [PubMed: 15292043]
37. Rohrer L, Hersberger M, Von Eckardstein A. High density lipoproteins in the intersection of diabetes mellitus, inflammation and cardiovascular disease. Current Opinion in Lipidology. 2004; 15 (3):269–278. [PubMed: 15166782]
38. Torres PA. Origin of the mediacalcosis in kidney failure. J Mal Vasc. May; 2009 34(3):204–10. [PubMed: 19345526]
39. Yoshikazu E, Koichi U, Ohnishi A, Ikushiro S, Iyanagi T. Transcriptional Enhancement of UDP-Glucuronosyltransferase Form 1A2 (UGT1A2) by Nuclear Factor I-A (NFI-A) in Rat Hepatocytes. Journal of Biochemistry. 2005; 138(3):313–325. [PubMed: 16169882]
40. Yurkova I, Kisel M. Free-radical fragmentation of galactocerebrosides: a MALDI-TOF mass spectrometry study. Chemistry and Physics of Lipids. Mar; 2005 134(1):41–49. [PubMed: 15752462]
41. Challen G, Gardiner B, Caruana G, Kostoulias X, Martinez G, Crowe M, Taylor DF, Bertram J, Little M, Grimmond SM. Temporal and spatial transcriptional programs in murine kidney development. Physiol Genomics. 2005; 17;23(2):159–7.
42. Guttmacher AE, Collins FS. Genomic medicine: a primer. N Engl J Med. 2002; 347:1512–1520. [PubMed: 12421895]
43. WU BX, Clarke CJ, Hannun YA. Mammalian Neutral Sphingomyelinases: Regulation and Roles in Cell Signaling Responses. Neuromolecular Med. 2010 Jun 16.
44. Landemaine T, Jackson A, Bellahcène A, Rucci N, Sin S, Abad BM, Sierra A, Boudinet A, Guinebretière JM, Ricevuto E, Noguès C, Briffod M, Bièche I, Cherel P, Garcia T, Castronovo V, Teti A, Lidereau R, Driouch K. A six-gene signature predicting breast cancer lung metastasis. Cancer Res. 2008; 68(15):6092–9. [PubMed: 18676831]
45. Barisoni L, Schnaper HW, Kopp JB. Advances in the biology and genetics of the podocytopathies: implications for diagnosis and therapy. Arch Pathol Lab Med. 2009; 133:201–216. [PubMed: 19195964]

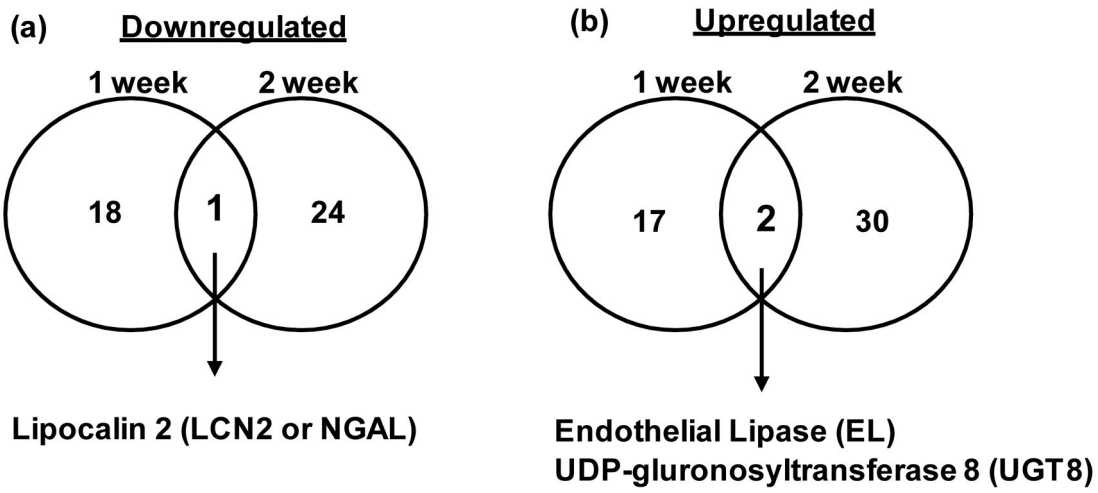

Figure 1.

Common genes (a) downregulated and (b) upregulated in podocytes cultured in high glucose for 1 and 2 weeks compared to normal glucose controls. Among the differentially expressed genes, only three were consistently altered at both time points. Refer to Table 1 for a detailed list of genes at each time point.

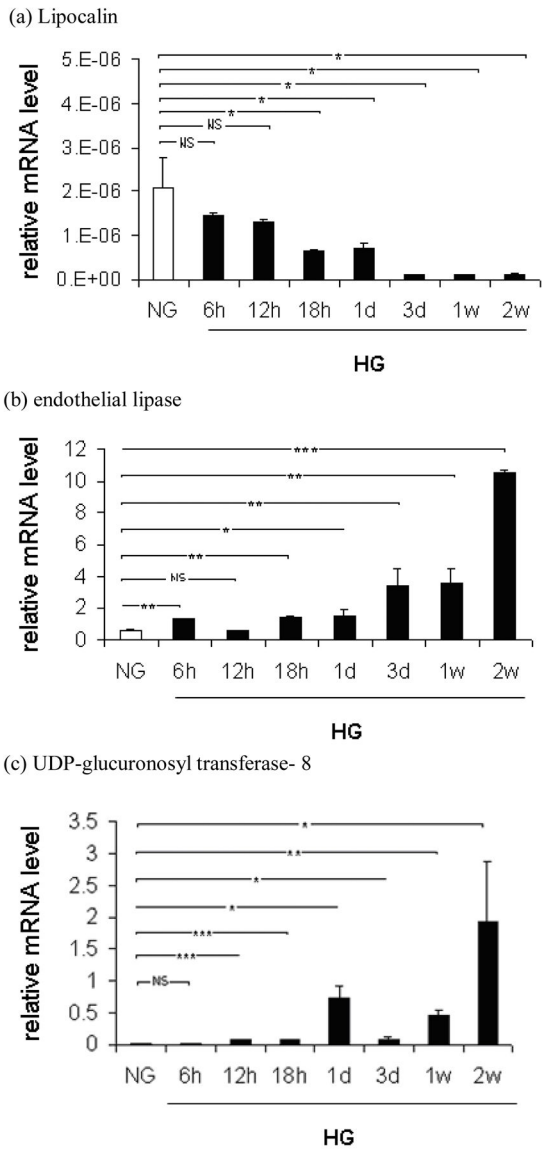

Figure 2.

Effect of high glucose on lipocalin (a), endothelial lipase (b) and UDP-glucuronosyl transferase- 8 (c) mRNA expression in podocytes. Cells were incubated in normal glucose RPMI 16 with/without 25 mM D-glucose for 6, 12, 18, 24, 48, 72 h, 1 week and 2 weeks. Cells were collected and assayed for target genes mRNA levels by real time-PCR . The relative mRNA expression of the target genes were normalized to β-actin control. Each point represents the mean SD of three independent experiments performed in triplicate. * *P* 0.05; ** *P* 0.01; *** *P* 0.001; NS, not significant.

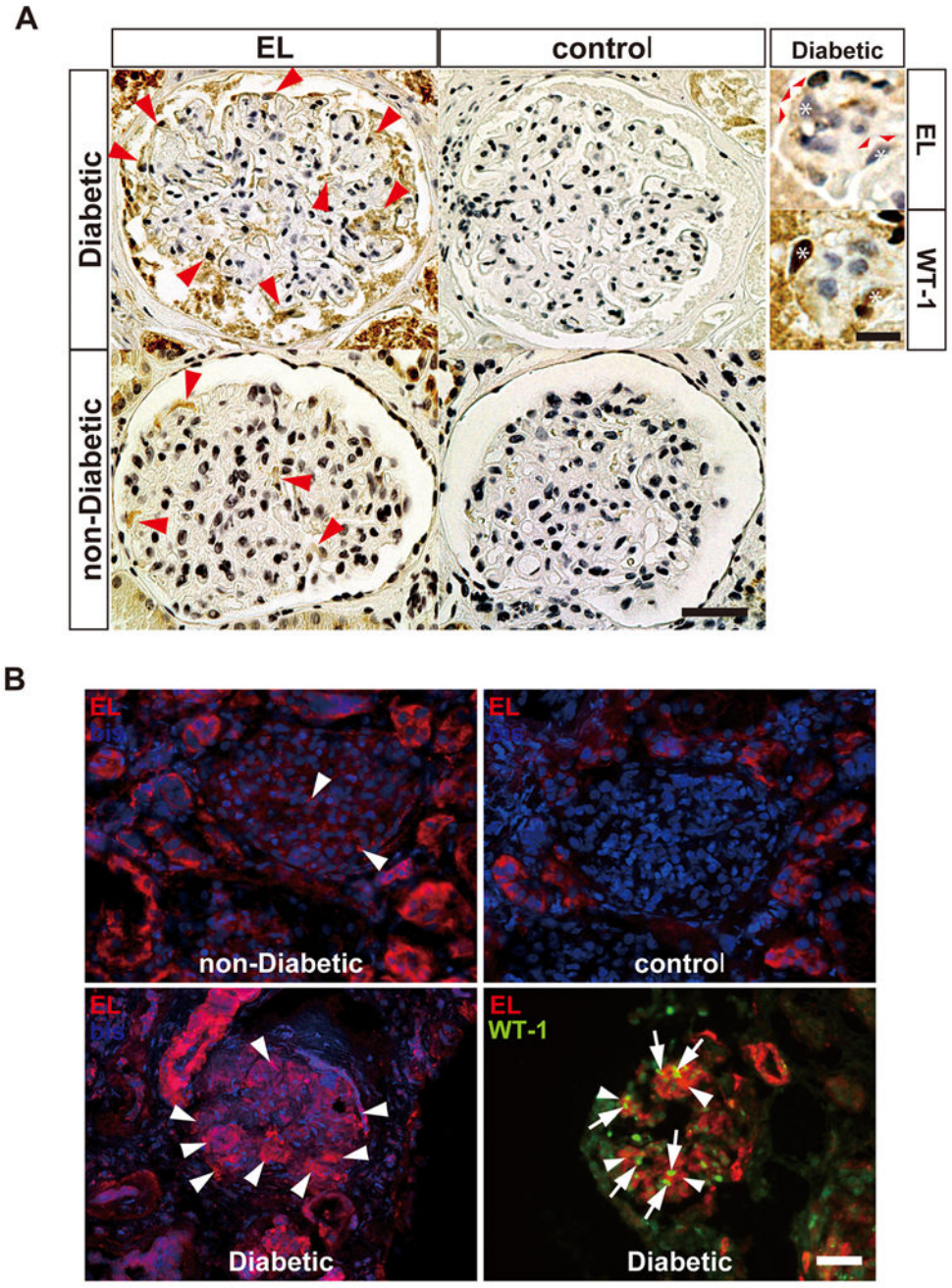

Figure 3.

High endothethelial lipase expression in kidney sections from diabetic patients compared to non-diabetic kidneys. Endothelial Lipase (EL) immunostaining was performed on formalin-fixed paraffin embedded (A) or cryopreserved biopsies (B) from patients with diabetic nephropathy (8) or non-diabetics (7) (see methods). The primary antibody was omitted in the control panel. All diabetic patients except one had increased EL immunopositivity in podocytes. Representative images from 3 diabetic and 2 non-diabetic patients are shown. (A) Immunoperoxidase staining (brown) with anti-EL antibodies show increased EL expression (red arrows) in podocytes and parietal cells of diabetic compared to non-diabetic

glomeruli. (scale bar = 50 μm). The high power images on the right (scale bar = 10 μm) are adjacent sections from a diabetic kidney stained with anti-EL or anti-WT-1 (as a podocyte marker) that show colocalization of EL (red arrowheads) and WT-1 (dark brown nuclear staining) in same cells (asterisks) supporting that EL and WT-1 are expressed in the podocytes. (B) EL immunofluorescence (red) on non-diabetic and diabetic kidney tissues also shows increased EL expression in diabetic glomeruli (lower panel), compared to non-diabetic glomeruli (upper panel). Control shows no glomerular staining. WT1 (green nuclear, arrowheads) immunostaining confirms that EL-expressing cells (arrows, cytoplasm) are podocytes. (scale bar = 50 μm). The tubulointerstitial staining is non-specific as it is present in controls in both A and B.

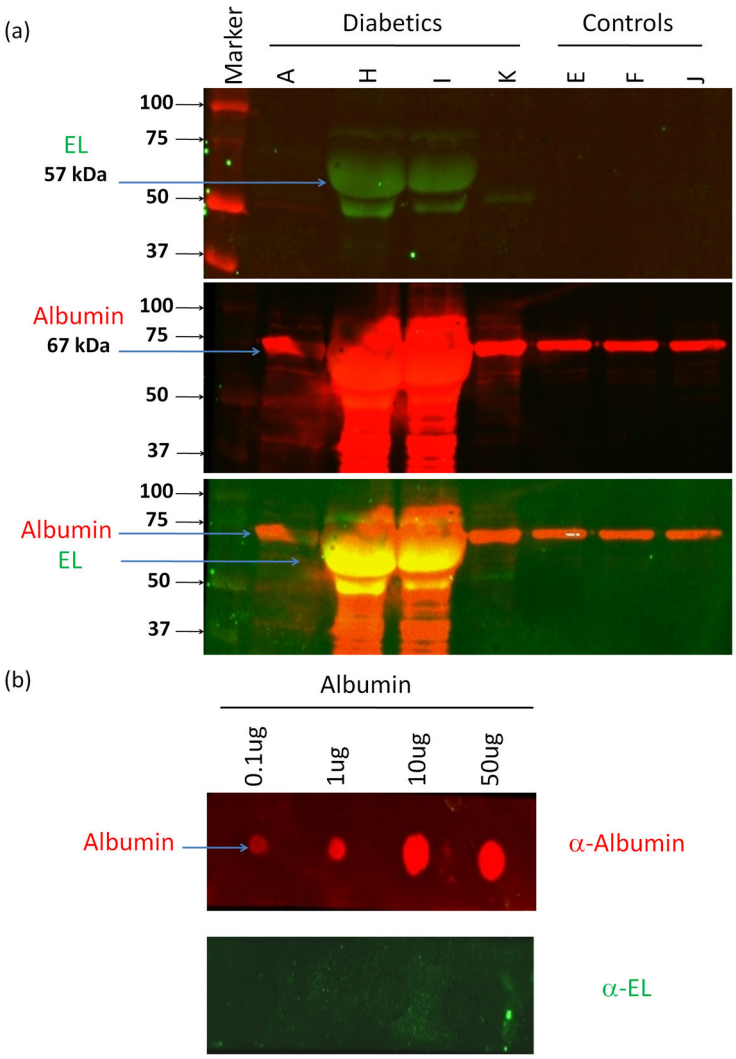

Figure 4.

Endothelial Lipase is readily detected in urine of diabetic nephropathy patients. (a) Immunoblot analysis for Endothelial Lipase (57KDa) (EL) and Albumin (67KDa) in urine samples of diabetic (lanes A, H, I and K) and non-diabetic controls (lanes E, F, and J). High levels of EL (green) are detected in urine samples of two diabetic patients (H and I). Controls show no EL excretion. Albumin (red) was detected in all samples. The lower panel shows distinct migration of EL and Albumin. (b) EL antibody does not cross react with albumin. Dot blot pattern of EL and Albumin immunostaining to different amounts of purified human albumin protein shows no immunostaining with EL antibody further confirming that EL detection is specific.

Table 1

Genes downregulated and upregulated in podocytes treated with high glucose for one week compared to podocytes cultured in normal glucose conditions. A cut off of 3 fold changes was used to filter the data (see methods).

Probe set	Downregulated gene	Accession	fold change
1448595_a_at	Bex1: brain expressed gene 1	NM_009052	−6.61
1458729_at	Mm.182696.1	AW552255	−5.32
1443153_at	Trip11: Thyroid hormone receptor interactor 11	BB306866	−4.21
1458269_at	Pcdh9: protocadherin 9	AW048370	−3.97
1427747_a_at	**Lcn2: lipocalin 2**	**X14607**	**−3.82**
1425339_at	Plcb4: phospholipase C, beta 4	BB224034	−3.6
1442704_at	Mm.214935.1	BM250739	−3.58
1450154_at	Folh1: folate hydrolase	NM_016770	−3.54
1445426_at	Mm.42287.1	BB457090	−3.36
1444229_at	Nr2f2: nuclear receptor subfamily 2, group F, member 2	BB053811	−3.34
1440488_at	Mm.209825.1	BB416028	−3.28
1425338_at	Plcb4: phospholipase C, beta 4	BB224034	−3.27
1444250_at	Mm.133185.1	AI451553	−3.23
1456659_at	LOC552902: hypothetical LOC552902	BM116906	−3.2
1424375_s_at	Gimap4: GTPase, IMAP family member 4	BC005577	−3.19
1439224_at	Mm.133637.1	BB373816	−3.17
1443145_at	Apbb1ip: amyloid beta (A4) precursor protein-binding, family B, member 1 interacting protein	BB153348	−3.12
1454589_at	9430006E15Rik: RIKEN cDNA 9430006E15 gene	AK020405	−3.08
1459750_s_at	Gpr123: G protein-coupled receptor 123	AU015577	−3.01
Probe set	**Upregulated gene**	**Accession**	**fold change**
1455930_at	Mm.28870.2	BI651113	8.2
1422317_a_at	Il1rl1: interleukin 1 receptor-like 1	NM_010743	5.59
1425843_at	Mrpl33: mitochondrial ribosomal protein L33	BC027018	4.88
1430786_at	1110002E22Rik: RIKEN cDNA 1110002E22 gene	BE991102	4.85
1449751_at	Slc6a6: Solute carrier family 6 (neurotransmitter transporter, taurine), member 6	AA589629	4.37
1435330_at	Pyhin1: pyrin and HIN domain family, member 1	BM241008	4.28
1437937_at	Ccbp2: chemokine binding protein 2	AV220666	4.13
1442844_at	A830052D11Rik: RIKEN cDNA A830052D11 gene	BB271008	3.86
1431315_at	Hyls1: hydrolethalus syndrome 1	BM570636	3.85
1447870_x_at	1110002E22Rik: RIKEN cDNA 1110002E22 gene	BB099116	3.81
1418676_at	Isl2: insulin related protein 2 (islet 2)	NM_027397	3.79
1444199_at	Mm.45087.1	AW046689	3.69
1425145_at	Il1rl1: interleukin 1 receptor-like 1	D13695	3.58
1422691_at	Sptlc1: serine palmitoyltransferase, long chain base subunit 1	AF003823	3.36
1421262_at	**Lipg: lipase, endothelial**	**BC020991**	**3.22**
1419063_at	**Ugt8a: UDP galactosyltransferase 8A**	**NM_011674**	**3.14**
1449356_at	Asb5: ankyrin repeat and SOCs box-containing 5	NM_029569	3.06

Probe set	Downregulated gene	Accession	fold change
1449473_s_at	Cd40: CD40 antigen	NM_011611	3.04
1439043_at	Tra2a: Transformer 2 alpha homolog (Drosophila)	BE982794	3.01

Table 2

Genes downregulated and upregulated in podocytes treated with high glucose for two week compared to podocytes cultured in normal glucose conditions. A cut off of 3 fold changes was used to filter the data (see methods).

probe set	Downregulated gene	Accession	fold change
1427747_a_at	**Lcn2: lipocalin 2**	**X14607**	**−7.03**
1459713_s_at	Ano1: anoctamin 1, calcium activated chloride channel	AU040576	−5.46
1434188_at	Slc16a12: solute carrier family 16 (monocarboxylic acid transporters), member 12	AV220703	−5.01
1419728_at	Cxcl5: chemokine (C-X-C motif) ligand 5	NM_009141	−4.49
1456078_x_at	Tubb2c /// Tubb2c-ps2: tubulin, beta 2C /// tubulin, beta 2c, pseudogene 2	BB012080	−4.32
1452014_a_at	Igf1: insulin-like growth factor 1	AF440694	−4.18
1423611_at	Alpl: alkaline phosphatase, liver/bone/kidney	AW319615	−4
1435603_at	Sned1: sushi, nidogen and EGF-like domains 1	BB487754	−3.91
1458536_at	Ccni: Cyclin I	BB097972	−3.69
1439364_a_at	Mmp2: matrix metallopeptidase 2	BF147716	−3.67
1448595_a_at	Bex1: brain expressed gene 1	NM_009052	−3.6
1454296_at	4631402F24Rik: RIKEN cDNA 4631402F24 gene	AA739023	−3.6
1450014_at	Cldn1: claudin 1	NM_016674	−3.5
1453550_a_at	Far1: fatty acyl CoA reductase 1	AK011187	−3.47
1449909_at	2010005H15Rik: RIKEN cDNA 2010005H15 gene	NM_029733	−3.44
1429951_at	Ssbp2: single-stranded DNA binding protein 2	AK005150	−3.36
1430097_at	8430436C05Rik: RIKEN cDNA 8430436C05 gene	AU016566	−3.35
1437405_a_at	Igfbp4: insulin-like growth factor binding protein 4	BB787243	−3.25
1459649_at	Mm.150125.1	AI662750	−3.23
1416441_at	Pgcp: plasma glutamate carboxypeptidase	BB468025	−3.16
1440107_at	Mm.131403.1	BB077622	−3.15
1421239_at	Il6st: interleukin 6 signal transducer	AA717838	−3.1
1429696_at	Gpr123: G protein-coupled receptor 123	BE946247	−3.1
1417625_s_at	Cxcr7: chemokine (C-X-C motif) receptor 7	BC015254	−3.09
1442254_at	Mm.207501.1	BB366659	−3.04
probe set	**Upregulated gene**	**Accession**	**fold change**
1455930_at	Mm.28870.2	BI651113	13.95
1419063_at	**Ugt8a: UDP galactosyltransferase 8A**	**NM_011674**	**5.26**
1444199_at	Mm.45087.1	AW046689	4.89
1431315_at	Hyls1: hydrolethalus syndrome 1	BM570636	4.59
1449751_at	Slc6a6: Solute carrier family 6 (neurotransmitter transporter, taurine), member 6	AA589629	4.57
1422944_a_at	Diap3: diaphanous homolog 3 (Drosophila)	NM_019670	4.46
1430786_at	1110002E22Rik: RIKEN cDNA 1110002E22 gene	BE991102	4.39
1426278_at	Ifi27l2a: interferon, alpha-inducible protein 27 like 2A	AY090098	4.37
1427184_at	Tcrb-J: T-cell receptor beta, joining region	BF318536	3.97
1421262_at	**Lipg: lipase, endothelial**	**BC020991**	**3.95**
1422155_at	Hist2h3c2: histone cluster 2, H3c2	BC015270	3.79

probe set	Downregulated gene	Accession	fold change
1455730_at	Dlgap5: discs, large (Drosophila) homolog-associated protein 5	BM250919	3.67
1441757_at	1190002F15Rik: RIKEN cDNA 1190002F15 gene	AI120476	3.65
1430419_at	2310031A07Rik: RIKEN cDNA 2310031A07 gene	AK009549	3.64
1421350_a_at	Grip1: glutamate receptor interacting protein 1	NM_130891	3.58
1439040_at	Cenpe: centromere protein E	BG068387	3.57
1447870_x_at	1110002E22Rik: RIKEN cDNA 1110002E22 gene	BB099116	3.57
1440862_at	Mm.153468.1	BB629079	3.44
1434847_at	Cnnm4: cyclin M4	BB432741	3.31
1421754_at	AY036118: cDNA sequence AY036118	NM_133243	3.3
1452458_s_at	Ppil5: peptidylprolyl isomerase (cyclophilin) like 5	BC022648	3.28
1417587_at	Timeless: timeless homolog (Drosophila)	BM230269	3.26
1449171_at	Ttk: Ttk protein kinase	NM_009445	3.26
1439510_at	Sgol1: shugoshin-like 1 (S. pombe)	BB410537	3.25
1417019_a_at	Cdc6: cell division cycle 6 homolog (S. cerevisiae)	NM_011799	3.23
1417938_at	Rad51ap1: RAD51 associated protein 1	BC003738	3.2
1452912_at	Dscc1: defective in sister chromatid cohesion 1 homolog (S. cerevisiae)	AK011162	3.17
1427004_at	Fbxo2: F-box protein 2	BB311718	3.09
1440146_at	Vps13a: vacuolar protein sorting 13A (yeast)	BB829606	3.09
1420707_a_at	Traip: TRAF-interacting protein	AK012948	3.06
1421881_a_at	Elavl2: ELAV (embryonic lethal, abnormal vision, Drosophila)-like 2 (Hu antigen B)	BB105998	3.06
1418480_at	Ppbp: pro-platelet basic protein	NM_023785	3

Table 3

Genes with altered expression both in 1W and 2W array datasets, compared to controls. Columns on the right represent the raw signal intensity data for the probesets for the indicated samples. The genes highlighted in bold were prioritized for validation based on consistency of replicate data across the arrays and available annotation.

probe set	gene	Accession	fold change	NG	NG	1W	1W	2W	2W
1419063_at	**Ugt8a: UDP galactosyltransferase 8A**	**NM_011674**	**5.26**	**353.8**	**163.9**	**881.9**	**715.9**	**1327**	**1251.9**
1421262_at	**Lipg: lipase, endothelial**	**BC020991**	**3.95**	**584.9**	**748.7**	**2338.1**	**1872.4**	**2285.2**	**2882.8**
1427747_a_at	**Lcn2: lipocalin 2**	**X14607**	**−7.03**	**5572.4**	**5442.6**	**1335.5**	**1546.3**	**958.8**	**563.5**
1430786_at	1110002E22Rik: RIKEN cDNA 1110002E22 gene	BE991102	4.39	531.2	467.5	2795.8	2011.6	1458.4	2842.1
1431315_at	Hyls1: hydrolethalus syndrome 1	BM570636	4.59	212.3	85.9	691.4	386.7	642.2	581.3
1444199_at	Mm.45087.1	AW046689	4.89	634.9	251	641.3	2593.8	555.9	3695.5
1447870_x_at	1110002E22Rik: RIKEN cDNA 1110002E22 gene	BB099116	3.57	1318.4	1917	6276.8	5591.4	3453	8163
1448595_a_at	Bex1: brain expressed gene 1	NM_009052	−3.6	8614.8	18678.4	3023.9	1035	6905.6	569.2
1449751_at	Slc6a6: Solute carrier family 6 (neurotransmitter transporter, taurine), member 6	AA589629	4.57	679.1	271.1	548	3369.7	820.2	3314.8
1455930_at	Mm.28870.2	BI651113	13.95	3317.7	2655.5	4788.1	49494.4	5569.2	89776